

**Supporting Information**

**High Pt-Mass Activity of Pt<sub>1</sub><sup>IV</sup>/β-MnO<sub>2</sub> Surface for  
Low-Temperature Oxidation of CO under O<sub>2</sub>-Rich Conditions**

Takeshi Nagata,<sup>[a]</sup> Akira Oda,<sup>\*[a,b]</sup> Yuta Yamamoto,<sup>[c]</sup> Risa Ichihashi,<sup>[a]</sup> Kyoichi Sawabe,<sup>[a,b]</sup> Atsushi Satsuma<sup>\*[a,b]</sup>

[a] Department of Materials Chemistry, Graduate School of Engineering, Nagoya University, Nagoya 464-8603, Japan.

[b] Elements Strategy Initiative for Catalysts and Batteries (ESICB), Kyoto University, Kyoto 615-8520, Japan.

[c] Institute of Materials and Systems for Sustainability, Nagoya University, Nagoya 464-8603, Japan.

Corresponding Authors

E-mail: akira@chembio.nagoya-u.ac.jp (A. O.); satsuma@chembio.nagoya-u.ac.jp (A. S.)

## 1. Methods

**1.1. Catalyst Preparation.**  $\beta$ -MnO<sub>2</sub> was synthesized by referring to a previous report.<sup>1</sup> NaMnO<sub>4</sub>•H<sub>2</sub>O ( $\geq 95\%$ , Sigma-Aldrich Co., LLC.) and MnSO<sub>4</sub>•5H<sub>2</sub>O ( $\geq 99.0\%$ , Kishida Chemical Co., Ltd.) were used as raw materials for Mn; 100 mL distilled water containing 7.25 g MnSO<sub>4</sub>•5H<sub>2</sub>O was stirred at 700 rpm, and 100 mL distilled water containing 3.15 g NaMnO<sub>4</sub>•H<sub>2</sub>O was added dropwise at a rate of 4.0 mL/min. The resulting suspension was further stirred at 700 rpm for 1 h. The precipitate was then collected by filtration, washed with water (10 L), dried at 80 °C overnight, and calcined at 400 °C for 5 h in air.

The Pt<sub>1</sub>/β-MnO<sub>2</sub> catalyst (Pt loading: 0.2 wt%) was prepared by the impregnation method; 8.6 wt% Pt(NO<sub>3</sub>)<sub>2</sub> aqueous solution (Cataler Co.) was used as the Pt source. After dispersion of the high-surface β-MnO<sub>2</sub> in 50 mL of water, a Pt(NO<sub>3</sub>)<sub>2</sub> aqueous solution was added dropwise and the mixture was stirred at room temperature for 1 h. The Pt was supported on the β-MnO<sub>2</sub> by removing the water with a rotary evaporator at 60 °C. The catalyst was dried at 80 °C for 12 h and calcined at 300 °C for 3 h in air. For comparison, Pt/β-MnO<sub>2</sub> catalysts with the higher Pt loadings (0.5, 2.0, 5.0, and 10 wt%) were also prepared by changing only the Pt amount in the above preparation method. Pt<sub>1</sub>/CeO<sub>2</sub> and Pt<sub>1</sub>/Fe<sub>2</sub>O<sub>3</sub> catalysts (Pt loading: 0.2 wt%) were prepared by the above impregnation method using CeO<sub>2</sub> (Catalysis Society of Japan, JRC-CEO-2) and Fe<sub>2</sub>O<sub>3</sub> (FUJIFILM Wako Co., Ltd.) as supports instead of β-MnO<sub>2</sub>.

**1.2. CO Oxidation Activity Test.** The CO oxidation tests were carried out in a fixed bed flow reactor at ambient pressure. The Pt<sub>1</sub>/β-MnO<sub>2</sub> catalyst (100 mg) was introduced into a U-shaped quartz tube (diameter: 100 mm, length: 35 cm) and fixed using quartz wool. After that, the catalyst was activated under 20% O<sub>2</sub>/Ar gas flow at 300 °C for 15 min. Then, the catalyst was cooled to the reaction temperature (0 °C or 25 °C), and subsequently exposed to the 0.3% CO–20% O<sub>2</sub>–79.7% Ar gas mixture with a total flow rate of 400 mL/min (240 L/g<sub>cat</sub>/h). The concentration of the CO<sub>2</sub> product was measured by general-purpose gas analyzers VA-3112 and VS-3003 (Horiba). The CO oxidation rate was calculated based on the concentration of the CO<sub>2</sub> product. To reduce the effect of the material and the thermal diffusion, the catalyst performance was evaluated under the reaction conditions where the CO conversion was less than 20% (Tables S3 and S4).

The long-term stability test showed that the initial catalytic activity is very high, but it decreased to half within the 0.5 h reaction, and becomes stable (Fig. S10). After that, the CO conversion gradually decreased with an increase in the reaction time. Activity-stability trade-off relation was observed. In the present study, the concentration of CO<sub>2</sub> at a reaction time of 2 hours was used for the calculation of Pt mass activity.

In the CO oxidation tests for the Pt/β-MnO<sub>2</sub> catalysts with the higher Pt loadings (0.5, 2.0, 5.0, and 10 wt%), the catalyst (50 mg) was mixed with SiC (50 mg), diluted, and used for the catalytic activity test.

**1.3. XRD.** XRD measurements were performed using a Rigaku ATX-G diffractometer (Rigaku) with Cu K $\alpha$  radiation. Data were collected in the  $2\theta$  range of 20–80° in 0.05° steps at a continuous scan rate of 1°/min<sup>-1</sup>.

**1.4. Brunauer–Emmett–Teller (BET) Surface Area Analysis.** The specific surface area of the catalysts was calculated by the BET method using N<sub>2</sub> gas. BELSORP-mini II (MicrotracBEL) was used for the analysis

of samples degassed at 200 °C for 1 h under vacuum.

#### 1.5. Scanning Electron Microscopy (SEM), Transmission Electron Microscopy (TEM), STEM.

SEM observations were carried out using a JSM-7500F (JEOL). TEM observations were carried out using a JEM-2100plus operating at 200 kV. STEM observations of the catalysts were performed using a JEM-ARM200FCs corrected S/TEM operating at 200 kV. TEM and STEM samples were prepared by spreading droplets of the catalyst water suspension on a Cu grid (200 mesh, EMJapan Co., Ltd.).

1.6. XPS. XPS measurements were performed with ESCALAB250Xi (Thermo Fisher Scientific) Al K $\alpha$  radiation. The sample was fixed to the sample table with carbon tape. The binding energy was calibrated to be 284.8 eV, which is the binding energy of C1s. XPSPEAK 4.1 software was used to analyze the data. A Shirley-type background was used to analyze the data.

1.7. XAFS Spectroscopy. Pt L<sub>III</sub>-edge XAFS measurements were performed in a Fluorescence mode at the BL5S1 beamline at the Aichi Synchrotron Radiation Center (Aichi, Japan). The disk sample (50 mg of Pt<sub>1</sub>/ $\beta$ -MnO<sub>2</sub> with the Pt loading of 0.2 wt%, 10 mm diameter) was transferred to the in-situ cell and activated by exposure to 20% O<sub>2</sub>/He at 300 °C for 15 min. After the pre-activation, the temperature was cooled to 25 °C, and then in situ XAFS measurement was performed for obtaining information on the geometric and electronic structures of the Pt single-atom sites before the reaction. Next, the catalyst was exposed to 0.3% CO–20% O<sub>2</sub>–79.7% He at a total flow rate of 200 mL/min (240 L/g<sub>cat</sub>/h) for 30 min, and then in situ XAFS measurement was carried out under the same conditions for obtaining information on the geometric and electronic structures of the Pt single-atom sites under the catalytic conditions. We have confirmed in advance that the catalytic activity is stable at least within 0.5–2 hours (Fig. S10); therefore, the in-situ XAFS measurement conditions are not so far from the actual catalytic conditions where the highest catalytic activity was observed. The XAFS data were analyzed using Athena and Artemis of the Demeter software package.<sup>2</sup> The FT-EXAFS spectrum was obtained through the FT of  $k^3\chi(k)$  function in the region  $3.0 < k < 12.0 \text{ \AA}^{-1}$ . The EXAFS fittings were performed on the  $q$ -space EXAFS functions obtained through the backward FT of the FT-EXAFS in the region  $1.3 R < 2.3 \text{ \AA}$ . Phases and backscattering amplitudes were calculated using the FEFF 6.0 code implemented in the Artemis software. The WT-EXAFS were drawn using the free software provided by ESRF<sup>3, 4</sup>, where the  $k^3\chi(k)$  function in the region  $3.0 < k < 12.0 \text{ \AA}^{-1}$  and WT parameters of  $\sigma = 1$  and  $\kappa = 7$  were used.

For comparison, the reference materials, i.e., 0.2 wt% Pt<sub>1</sub>/CeO<sub>2</sub> and Pt<sub>1</sub>/Fe<sub>2</sub>O<sub>3</sub>, were also characterized by extu XAFS measurements in a Fluorescence mode at the BL01B1 beamline at SPring-8 (Hyogo, Japan). The FT-EXAFS spectra were obtained through the FT of  $k^3\chi(k)$  functions in the region of  $3.0 < k < 11.0 \text{ \AA}^{-1}$ .

## 2. Supporting Data

**Table S1.** BET surface area, pore volume, and pore diameter of  $\beta$ -MnO<sub>2</sub> and Pt<sub>1</sub>/ $\beta$ -MnO<sub>2</sub>.

| Catalyst                                    | BET surface area (m <sup>2</sup> /g) | Pore volume (cm <sup>3</sup> /g) | Pore diameter (nm) |
|---|--------------------------------------|----------------------------------|--------------------|
| $\beta$ -MnO <sub>2</sub>                   | 150                                  | 0.0848                           | 2.25               |
| Pt <sub>1</sub> / $\beta$ -MnO <sub>2</sub> | 116                                  | 0.0655                           | 2.26               |

**Table S2.** Structural information of the Pt<sup>IV</sup> single-atom sites of Pt<sub>1</sub>/ $\beta$ -MnO<sub>2</sub>, extracted by the best fit  $k^3\chi(k)$  function of Pt L<sub>III</sub>-edge EXAFS spectrum assuming Pt–O backscattering in the range of  $1.3 R < 2.3 \text{ \AA}$ .

| Backscattering | <i>C. N.</i> | <i>R</i> (Å) | $\sigma^2 \times 10^3$ (Å <sup>2</sup> ) | R-factor |
|----------------|--------------|--------------|--|----------|
| Pt–O           | 6.1±1.3      | 2.04±0.01    | 2.92±1.57                                | 0.0096   |

**Table S3.** Reaction rates of CO oxidation at 25 °C over Pt/ $\beta$ -MnO<sub>2</sub> with a variety of Pt-loadings. Reaction condition: 0.3% CO–20% O<sub>2</sub>–79.7% Ar, with a total flow rate of 400 mL/min (240 L/g<sub>cat</sub>/h), 100 mg catalyst.

| Pt loading (wt%) | Reaction rate (mol <sub>CO</sub> /h/g <sub>Pt</sub> ) | CO conversion (%) |
|------------------|---|-------------------|
| 0.2              | 0.676   | 4.22              |
| 0.5              | 0.448   | 3.49              |
| 2.0              | 0.322   | 10.1              |
| 5.0              | 0.182   | 14.2              |
| 10.0             | 0.119   | 18.6              |

**Table S4.** Pt loading, BET surface area, and reaction rate at 25 °C for Pt<sub>1</sub><sup>IV</sup>/ $\beta$ -MnO<sub>2</sub>, Pt<sub>1</sub>/Fe<sub>2</sub>O<sub>3</sub>, and Pt<sub>1</sub>/CeO<sub>2</sub>. Reaction condition: 0.3% CO–20% O<sub>2</sub>–79.7% Ar, with a total flow rate of 400 mL/min (240 L/g<sub>cat</sub>/h), 100 mg catalyst.

| Catalyst  | Pt loading (wt%) | BET surface area (m <sup>2</sup> /g) | Reaction rate (mol <sub>CO</sub> /h/g <sub>Pt</sub> ) | CO conversion (%) |
|---|------------------|--------------------------------------|---|-------------------|
| Pt <sub>1</sub> <sup>IV</sup> / $\beta$ -MnO <sub>2</sub> | 0.2              | 116                                  | 0.676   | 4.22              |
| Pt <sub>1</sub> /CeO <sub>2</sub>                         | 0.2              | 122                                  | 0   | 0                 |
| Pt <sub>1</sub> /Fe <sub>2</sub> O <sub>3</sub>           | 0.2              | 32.7                                 | 0.042   | 0.45              |

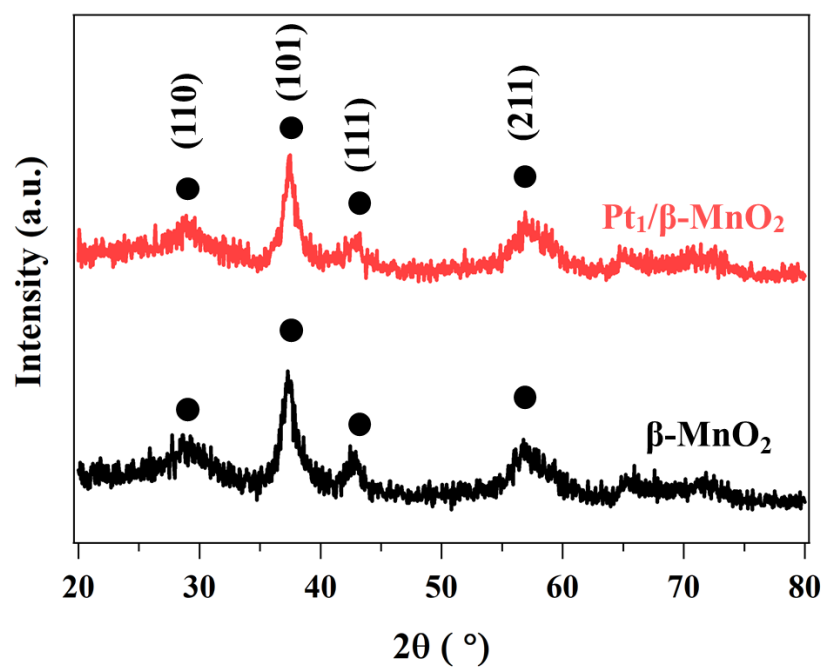
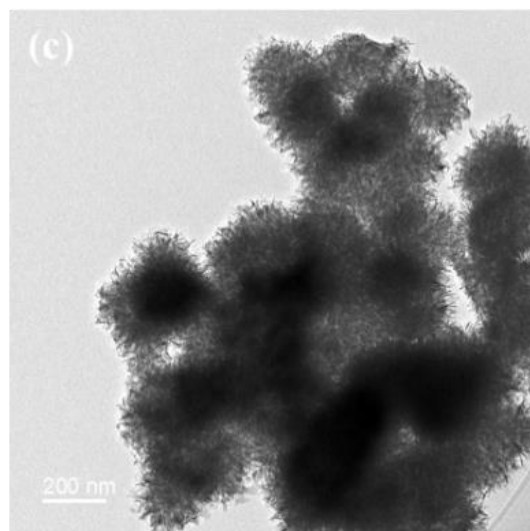
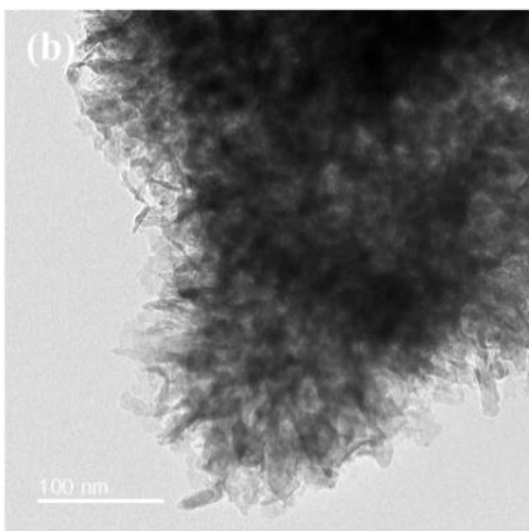
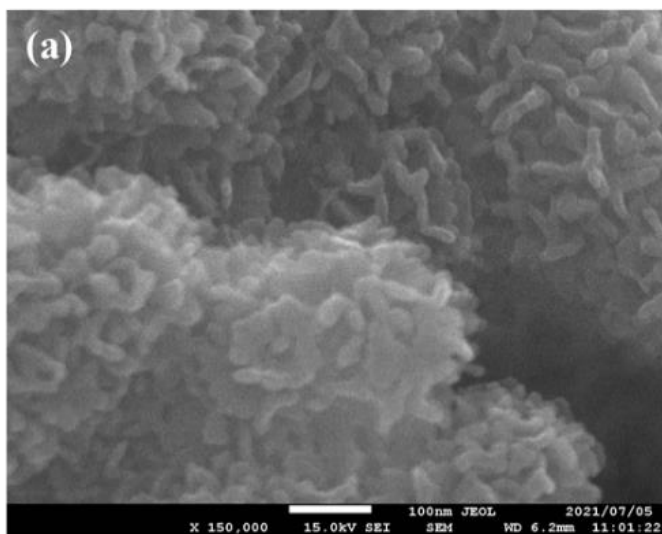
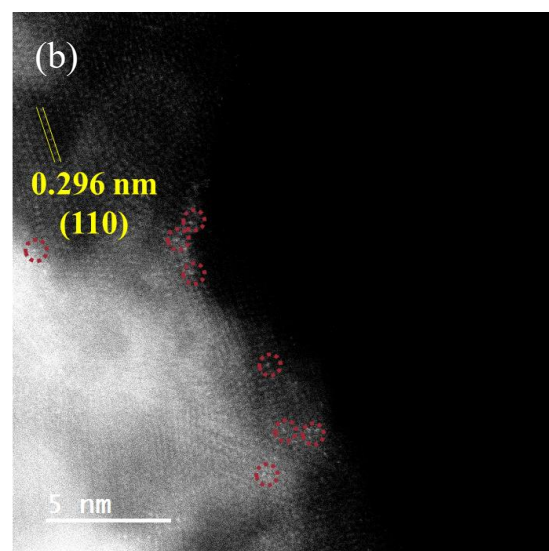
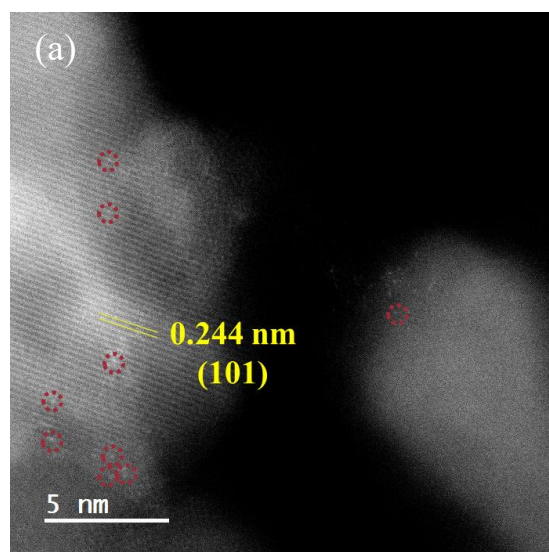


Fig. S1 XRD patterns for  $\beta\text{-MnO}_2$  and  $\text{Pt}_1/\beta\text{-MnO}_2$ .



**Fig. S2** (a) SEM and (b, c) TEM images of the  $\beta$ - $\text{MnO}_2$  support.



**Fig. S3** Additional HAADF-STEM images of Pt<sub>1</sub>/ $\beta$ -MnO<sub>2</sub> catalysts.

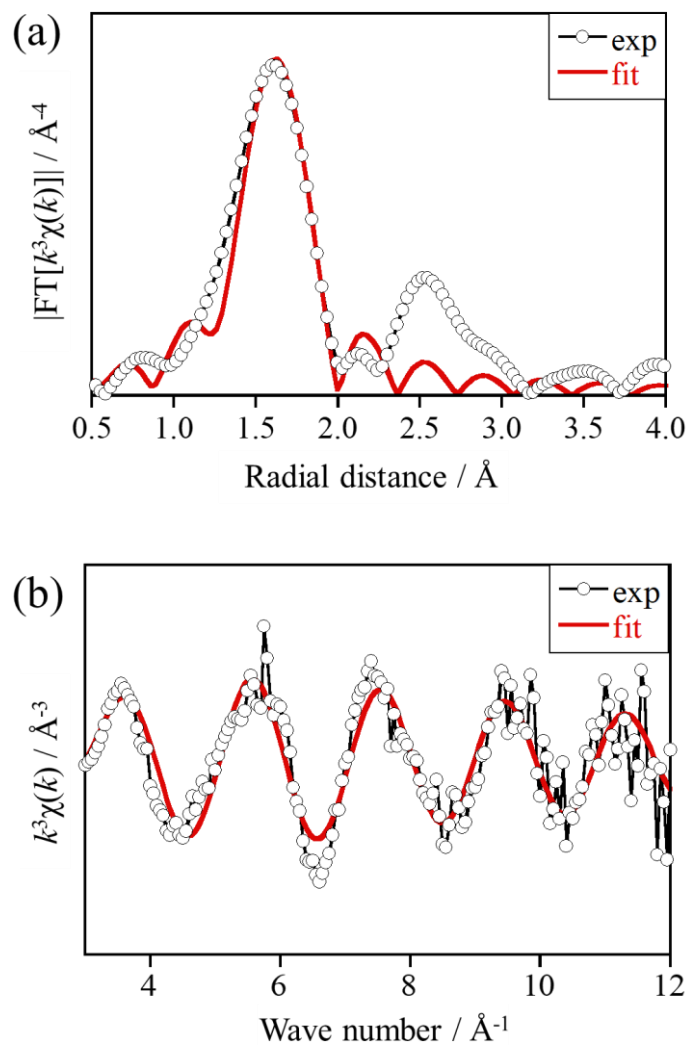


**Fig. S4** EXAFS fitting results for Pt<sub>1</sub>/β-MnO<sub>2</sub>. (a) The experimental  $k^3\chi(k)$  function with the best fit function. (b) Phase uncorrected  $R$ -space EXAFS spectra obtained through the FT of the  $k^3\chi(k)$  function in a range of  $3.0 < k < 12.0 \text{ Å}^{-1}$  with the best-fit spectra. For the EXAFS fitting, only Pt–O backscattering was considered.



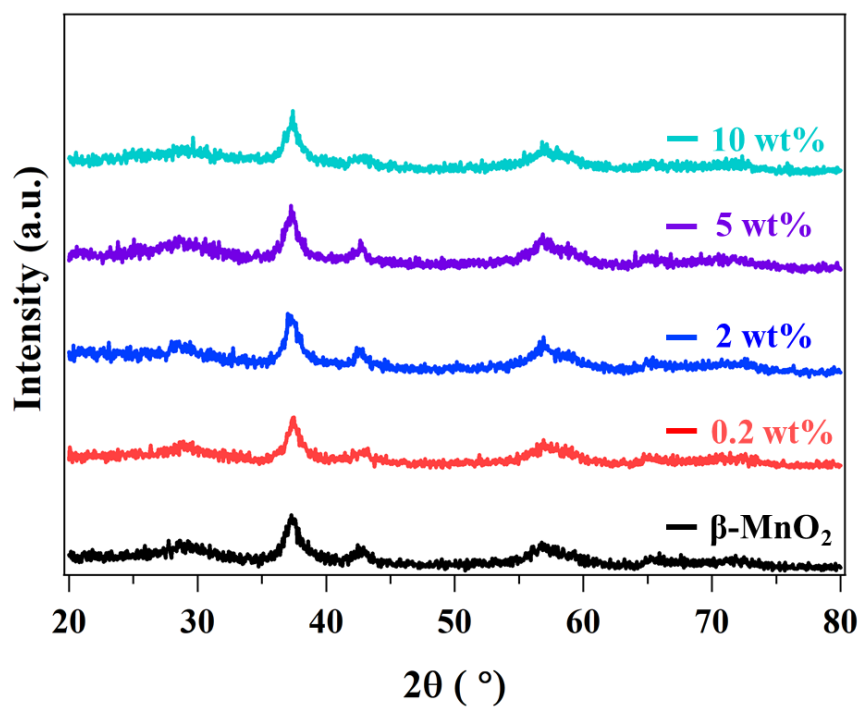


**Fig. S5** XRD profiles of Pt/ $\beta$ -MnO<sub>2</sub> with the Pt loading of 0.2 wt%, 2 wt%, 5 wt%, 10 wt%. For comparison, the XRD profile of Pt-free  $\beta$ -MnO<sub>2</sub> was also given.

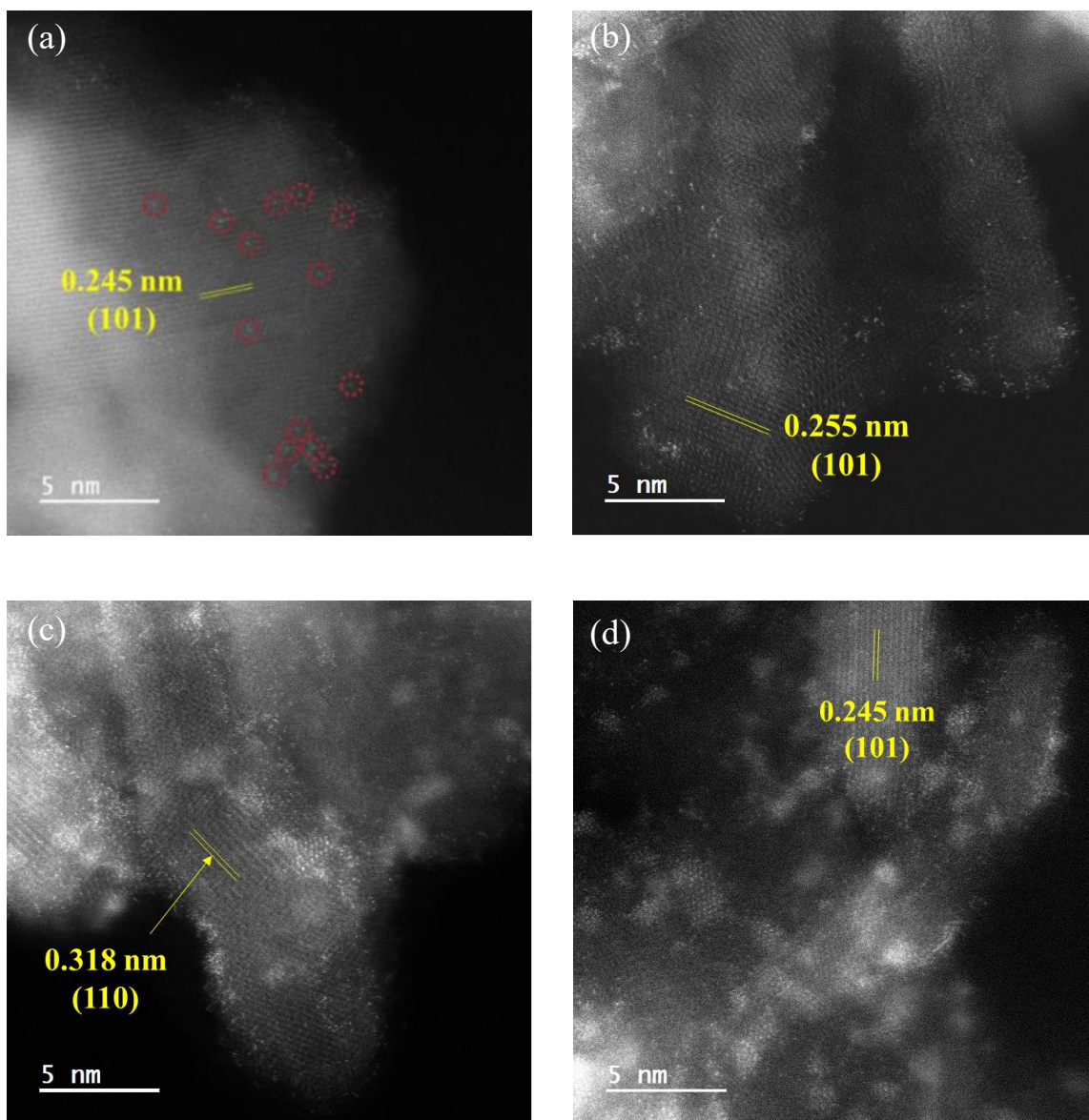


**Fig. S6** HAADF-STEM images of Pt/ $\beta$ -MnO<sub>2</sub> catalysts with the Pt loadings of (a) 0.2 wt%, (b) 2 wt%, (c) 5 wt%, and (d) 10 wt%.

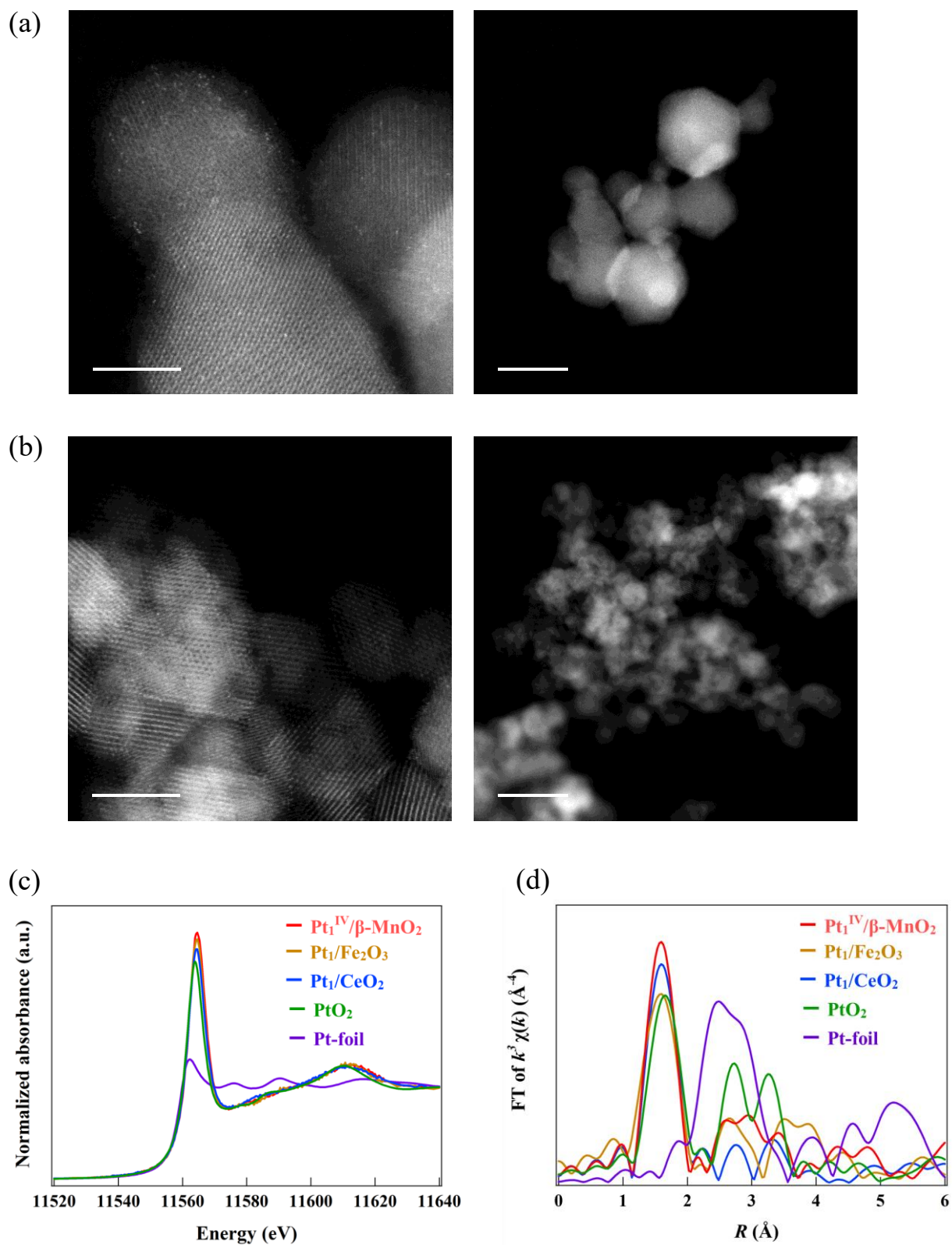


**Fig. S7** (a-d) HAADF-STEM images of (a) 0.2 wt% Pt<sub>1</sub>/Fe<sub>2</sub>O<sub>3</sub> and (b) Pt<sub>1</sub>/CeO<sub>2</sub>. Pt L<sub>III</sub>-edge (c) XANES and (d) FT-EXAFS spectra for Pt<sub>1</sub>/Fe<sub>2</sub>O<sub>3</sub>, and Pt<sub>1</sub>/CeO<sub>2</sub>. For references, the related data of Pt<sub>1</sub>/β-MnO<sub>2</sub> with the Pt loading of 0.2 wt%, Pt foil and PtO<sub>2</sub> were also given.

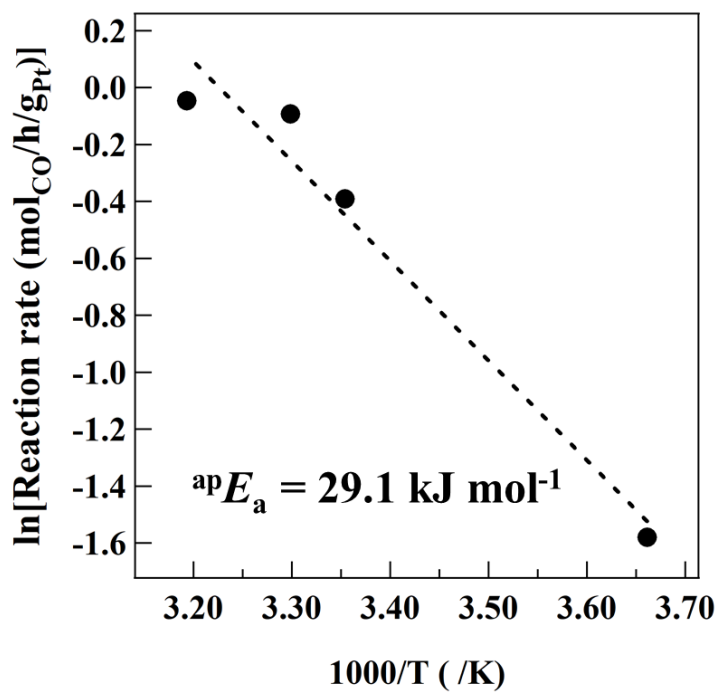


**Fig. S8** Dependencies of the reaction rates of CO oxidation over  $\text{Pt}_1^{\text{IV}}/\beta\text{-MnO}_2$  on the reaction temperature. Reaction condition: 0.3%  $\text{CO}$ –20%  $\text{O}_2$ –79.7%  $\text{Ar}$ , with total flow rate of 400 mL/min (240 L/g<sub>cat</sub>/h), 100 mg catalyst.

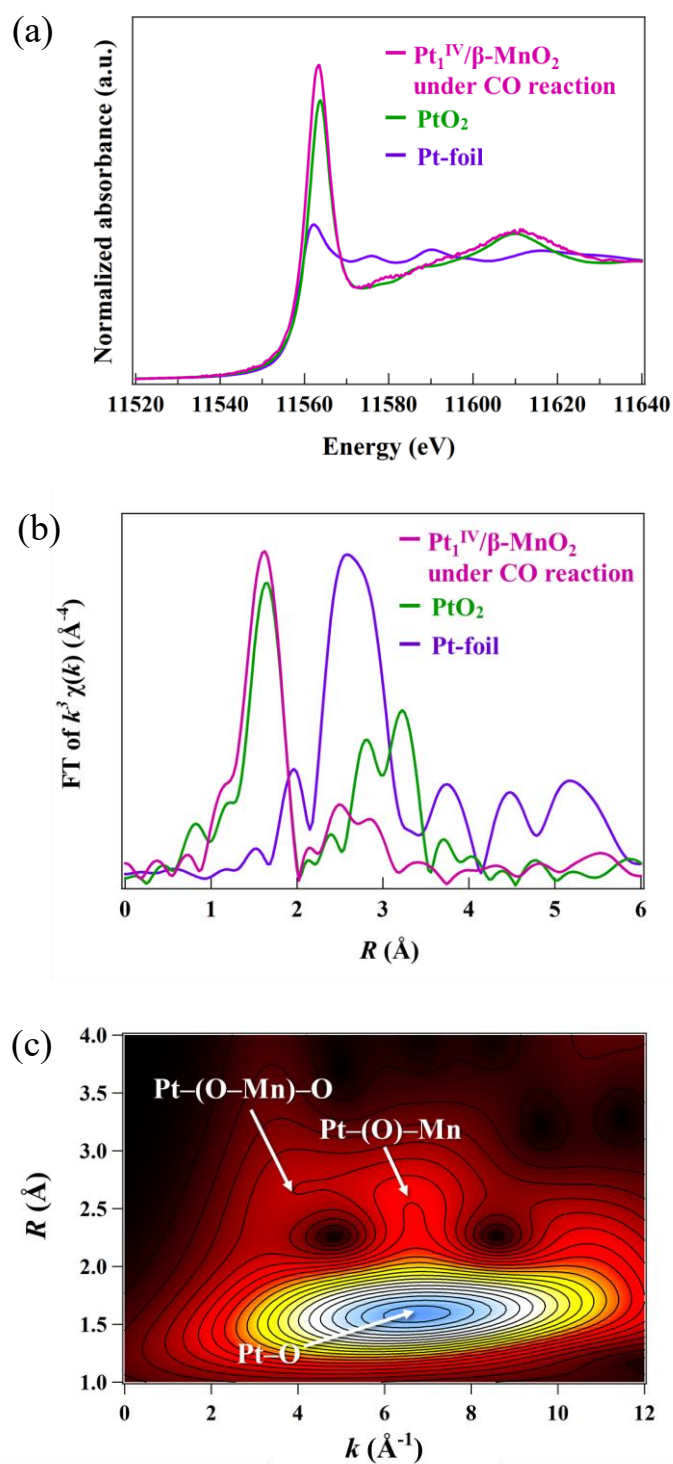


**Fig. S9** In-situ XAFS characterizations of the Pt<sub>1</sub><sup>IV</sup>/β-MnO<sub>2</sub> catalyst under the CO reaction condition: (a) XANES, (b) FT-EXAFS, and (c) WT-EXAFS. The reaction was conducted in a gas mixture of 0.3% CO–20% O<sub>2</sub>–79.7% He with a total flow rate of 200 mL/min (240 L/g<sub>cat</sub>/h) at an ambient pressure at 25 °C, where 50 mg catalyst was used. For comparison, the XANES and FT-EXAFS of PtO<sub>2</sub> and Pt-foil are also given.

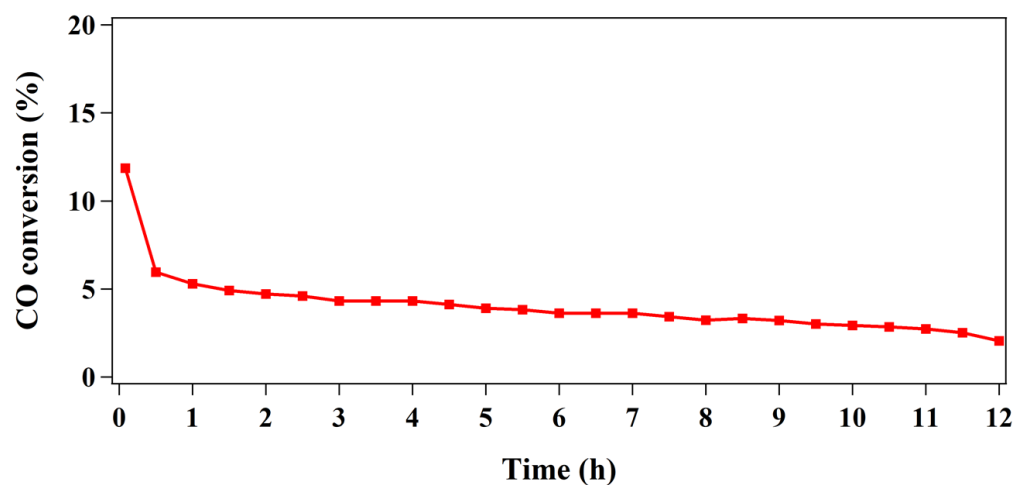


**Fig. S10** Long term stability test for Pt/ $\beta$ -MnO<sub>2</sub> with the Pt loading of 0.2 wt%. Reaction condition: 0.3% CO–20% O<sub>2</sub>–79.7% Ar, with a total flow rate of 400 mL/min (240 L/g<sub>cat</sub>/h), 100 mg catalyst.

### 3. Supporting References

- [1] E. Hayashi et al. *J. Am. Chem. Soc.*, 2019, **141**, 899–900.
- [2] B. Ravel, M. Newville, *Phys. Scr.*, 2005, **T115**, 1007–1010.
- [3] H. Funke, A. Scheinost, M. Chukalina, *Phys. Rev. B*, 2005, **71**, 094110.
- [4] H. Funke, M. Chukalina, A. C. Scheinost, *J. Synchrot. Radiat.*, 2007, **14**, 426–432.